

Stability of Schwarzschild- $f(R)$ gravity thin-shell wormholes

Alina Khaybullina* and Gulira Tuleganova†

Zel'dovich International Center for Astrophysics, Bashkir State Pedagogical University,
3A, October Revolution Street, Ufa 450008, RB, Russia

(Dated: August 31, 2021)

Mazharimousavi and Halilsoy [1] recently proposed wormhole solutions in $f(R)$ -gravity that satisfy energy conditions but are unstable. We show here that stability could still be achieved for thin-shell wormholes obtained by gluing the wormholes in $f(R)$ -gravity with the exterior Schwarzschild vacuum. Using the new geometrical constraints from thin-shell "mass" and from external "force" developed by Garcia, Lobo and Visser, we demarcate and analyze the stability regions.

I. INTRODUCTION

Wormholes are geometrical handles in spacetime that connect two universes or two distant regions of spacetime and are solutions of Einstein's general relativity including other theories of gravity. The subject has received considerable attention after the influential theoretical work by Morris and Thorne [2]. While there exist enormous work on black holes, especially directed to observing the signatures of a supermassive black hole at our galactic center, relatively less work is available on wormholes. This scenario has now drastically changed due to the recent discovery that thin-shell wormholes have the ability to mimic recently observed gravitational ring-down post-merger waves that have heretofore been believed to be characteristic exclusively of black hole horizon [3-6]. Therefore, the study of stability of thin-shell wormholes is of paramount importance.

Morris-Thorne wormholes within Einstein's theory of general relativity (GR) require exotic ghost matter (i.e., matter that violates the Null Energy Condition ¹) for their construction, as shown by Hochberg and Visser [7]. While all experiments to date have failed to directly detect astrophysical ghost matter, modified gravity theories such as the $f(R)$ -gravity (where R is the Ricci scalar) seems to provide a promising avenue to look at gravitational from a more general perspective beyond Einstein's theory (for which $f(R) = R$). There exist extensive works on black holes and wormholes in $f(R)$ -gravity. Some key references, though by no means exhaustive, might be mentioned, see e.g., [8-12]. Excellent reviews on $f(R)$ -gravity are also available [13-16].

On the state-of-the-art of $f(R)$ -gravity, a thorough update on the existence, stability and thermodynamics of different configurations is in order. The existence problem concerns the conditions necessary for the existence of configurations in $f(R)$ -gravity that are analogous to the ones in GR. The strategy to obtain those conditions is to employ what is called a *near-horizon test* in [17,18] exploiting the regularity of GR black hole horizon. The regularity allows the metric functions to be analytically expanded around the horizon and when they are put back in the field equations of $f(R)$ -gravity, they yield the necessary conditions on the form of $f(R)$ admitting analog black holes or $f(R)$ -black holes. The remarkable result obtained in [17,18] is that just any arbitrary *polynomial* form of $f(R)$ do not admit analog black holes. A classic example is that the existence of analog Schwarzschild black hole requires that $f(R)$ -gravity must be of the specific form $f(R) = \alpha\sqrt{R+\beta}$, where α, β are constants. Analog Reissner-Nordström black hole requires an infinite series form of $f(R)$ with the coefficients determined by the horizon radius [19].

As to the question of stability, a viable $f(R)$ -gravity solution should be stable, ghost-free and should admit Newtonian and Post-Newtonian limits including correct cosmological dynamics. This means that for the stability of analog black holes, the near-horizon test yielding the form of $f(R)$ should be further constrained by the conditions that $\frac{df}{dR} > 0$ and $\frac{d^2f}{dR^2} > 0$ [19]. From a different viewpoint, Myung, Moon and Son [20] converted the $f(R)$ -gravity into a Brans-Dicke theory with massive scalaron and showed that the $f(R)$ analog of Schwarzschild black hole is stable against the external perturbations if the scalaron mass squared is not negative (tachyonic mass) that is ensured by the condition $\left. \frac{d^2f}{dR^2} \right|_{R=0} > 0$. The opposite of this stability inequality is the Dolgov-Kawasaki instability condition $\frac{d^2f}{dR^2} < 0$ applicable to perturbations in several distinct spacetimes [21-25]. Instability of analog Kerr black holes in $f(R)$ -gravity has also been studied [26]. The status of Jepsen-Birkoff theorem and its stability in $f(R)$ -gravity has been studied in [27].

*Electronic address: kalina89-rf@mail.ru

†Electronic address: gulira.tuleganova@yandex.ru

¹ That is, matter having $\rho + p_r < 0$, $\rho + p_t < 0$, where ρ is the energy density, p_r and p_t are radial and transverse components of pressure.

Thermodynamics of analog black holes have been studied [19,28-31]. In [28], using the Hawking temperature and entropy, the exact expression for heat capacity and the first law of thermodynamics have been found by using the Misner-Sharp formalism [19]. Similar thermodynamics dealing with analog Reissner-Nordström black hole also exists [29]. Another novel method of studying thermodynamics and phase transitions of analog black holes is to use geometrothermodynamical methods [30]. Yokokura [31] generalized the space-time thermodynamics and then from the equation for entropy balance for nonequilibrium processes found the new entropy production terms in $f(R)$ -gravity.

Wormhole solutions including the thin-shell variants have also been obtained in $f(R)$ -gravity [1,32]. Evolving wormholes have been recently found by Bhattacharya and Chakraborty [33]. Wormholes in the Palatini formulation of $f(R)$ gravity have been studied in [34]. Necessary conditions for having wormholes in $f(R)$ -gravity have been obtained in [35]. Some thin-shell wormholes and their stabilities have been studied in [36-38]. The focus in this paper is on the two traversable analytical wormhole solutions recently found by Mazharimousavi and Halilsoy (MH) [1]. These wormholes are however unstable since, as generically argued in [39], there cannot be ghost-free, stable wormholes in $f(R)$ -gravity. This being the case, it would be of interest to study the possibility of stability of thin-shell wormholes obtained by gluing the exterior Schwarzschild vacuum with MH wormholes of $f(R)$ -gravity².

In this Letter, our purpose is to use the new constraints developed by Garcia, Lobo and Visser (GLV) [40] for identifying the stability regions of the linearly perturbed spherical motion of the thin-shell moving in the bulk spacetime. For this purpose, we obtain the thin-shell by gluing the relevant solutions at some suitable "standard" coordinate radius. In other words, the asymptotic masses on one side will be the mass of the wormhole in $f(R)$ -gravity and on the other side the Schwarzschild mass. Henceforth, we take $G = 1, c = 1$ unless specifically restored.

II. GLV FORMALISM FOR STABILITY

This formalism being relatively new, for the benefit of readers, we explain below in slightly more detail the GLV formalism [40] for stability of the thin-shell and the attendant new concepts. The formalism is quite generic, flexible and robust that can be applied to general spherically symmetric spacetimes in 4-dimensions. The idea is to surgically graft together two bulk spacetimes in such a way that no event horizon is formed. This surgery generates a thin shell (the wormhole throat, where all the exotic matter is concentrated) between the two bulk spacetimes on either side of the throat. The thin shell will be free to move in the bulk spacetimes allowing a fully dynamic stability analysis against spherically symmetric perturbations. The stability will then be dictated by the properties of the exotic matter residing on the wormhole throat. The novelty of the formalism is that, apart from a "mass" constraint from the mass of the shell, it introduces an entirely *new* hitherto unknown geometrical constraint of external "force". The motion of the shell is driven by a "potential" $V(a)$ appearing in the equation of motion $\frac{1}{2}\dot{a}^2 + V(a) = 0$ and the stability under small oscillation about a static solution $a = a_0$ (initial gluing radius) will be given by the condition $V''(a_0) \geq 0$. This is, in short, the strategy of GLV formalism.

We note that GLV method is developed within Einstein's GR having second order equations, whereas $f(R)$ -gravity equations are of fourth order. To justify the use of GLV method gluing the two solutions from two different theories, we recall the conformal equivalence of $f(R)$ -gravity with GR minimally coupled to a scalar field with a potential. Mathematically, the conformal transformation converts the fourth-order $f(R)$ equations into two second-order equations, one for the Einstein frame metric and the other for a scalar field φ . The needed junction condition on extrinsic curvature in the Einstein frame is the same as in GR [41].

Omitting lengthy details, we shall try to reproduce the salient features of GLV formalism as cogently as possible, especially the steps leading to the usable stability constraints. The method starts with gluing together two spherically symmetric spacetimes by "cut and paste" surgery developed by Visser [42]. GLV take two generic spherically symmetric spacetimes \mathcal{M}_\pm possessing the metrics in each as

$$ds_\pm^2 = -e^{2\Phi_\pm(r_\pm)} \left[1 - \frac{b_\pm(r_\pm)}{r_\pm} \right] c^2 dt_\pm^2 + \left[1 - \frac{b_\pm(r_\pm)}{r_\pm} \right]^{-1} dr_\pm^2 + r_\pm^2 d\Omega_\pm^2, \quad (1)$$

where $\Omega = d\theta^2 + \sin^2 \theta d\phi^2$. A single manifold \mathcal{M} is obtained by gluing the two manifolds \mathcal{M}_+ and \mathcal{M}_- at Σ , i.e., at $f(r, \tau) = r - a(\tau) = 0$. That is, the points $r < a(\tau)$ are excised out of \mathcal{M} and the intrinsic metric on Σ is assumed to have a form

$$ds_\Sigma^2 = -d\tau^2 + a(\tau)^2 (d\theta^2 + \sin^2 \theta d\phi^2). \quad (2)$$

² As appropriately commented by an anonymous referee, the present Letter provides a "graceful exit" to the usual wormhole instabilities.

The position of the junction surface is given by $x^\mu(\tau, \theta, \phi) = [t(\tau), a(\tau), \theta, \phi]$, and the non-trivial extrinsic curvature components on both sides of the shell are given by

$$K^\theta_\theta^\pm = \pm \frac{1}{a} \sqrt{1 - \frac{b_\pm(a)}{a} + \dot{a}^2}, \quad (3)$$

$$K^\tau_\tau^\pm = \pm \left\{ \frac{\ddot{a} + \frac{b_\pm(a) - b'_\pm(a)a}{2a^2}}{\sqrt{1 - \frac{b_\pm(a)}{a} + \dot{a}^2}} + \Phi'_\pm(a) \sqrt{1 - \frac{b_\pm(a)}{a} + \dot{a}^2} \right\}, \quad (4)$$

where the prime now denotes a derivative with respect to the coordinate a and overdot denotes derivative with respect to τ . Note that K_{ij} is not continuous across Σ , so one defines $\kappa_{ij} = K_{ij}^+ - K_{ij}^-$ that satisfy Lanczos equations on the shell as

$$S^i_j = -\frac{1}{8\pi} (\kappa^i_j - \delta^i_j \kappa^k_k), \quad (5)$$

where S^i_j is the surface stress-energy tensor on Σ defined by $S^i_j = \text{diag}(-\sigma, \mathcal{P}, \mathcal{P})$, σ is the surface energy density and \mathcal{P} is the surface pressure

$$\sigma = -\frac{1}{4\pi a} \left[\sqrt{1 - \frac{b_+(a)}{a} + \dot{a}^2} + \sqrt{1 - \frac{b_-(a)}{a} + \dot{a}^2} \right], \quad (6)$$

$$\begin{aligned} \mathcal{P} = \frac{1}{8\pi a} & \left[\frac{1 + \dot{a}^2 + a\ddot{a} - \frac{b_+(a) + ab'_+(a)}{2a}}{\sqrt{1 - \frac{b_+(a)}{a} + \dot{a}^2}} + \sqrt{1 - \frac{b_+(a)}{a} + \dot{a}^2} a\Phi'_+(a) \right. \\ & \left. + \frac{1 + \dot{a}^2 + a\ddot{a} - \frac{b_-(a) + ab'_-(a)}{2a}}{\sqrt{1 - \frac{b_-(a)}{a} + \dot{a}^2}} + \sqrt{1 - \frac{b_-(a)}{a} + \dot{a}^2} a\Phi'_-(a) \right]. \end{aligned} \quad (7)$$

The surface stress S^i_j satisfies a conservation identity via Lanczos and Gauss-Codazzi equation as

$$S^i_{j|i} = [T_{\mu\nu} e^\mu_{(j)} n^\nu]^+_- , \quad (8)$$

where n^ν is the unite normal to Σ and $e^\mu_{(j)}$ are the orthonormal basis vectors such that $g_{ij} = g_{\mu\nu} e^\mu_{(i)} e^\nu_{(j)}|_\pm$. Defining a new term

$$\Xi = \frac{1}{4\pi a} \left[\Phi'_+(a) \sqrt{1 - \frac{b_+(a)}{a} + \dot{a}^2} + \Phi'_-(a) \sqrt{1 - \frac{b_-(a)}{a} + \dot{a}^2} \right], \quad (9)$$

the conservation identity (8) can be written as

$$\frac{d(\sigma A)}{d\tau} + \mathcal{P} \frac{dA}{d\tau} = \Xi A \dot{a}, \quad (10)$$

where $\dot{a} = \frac{da}{d\tau}$, $A = 4\pi a^2$ is the surface area of the shell. The first term represents change in the internal energy of the shell, while the second term represents the work done by the shell's internal force, and the third term represents the work done by the external forces (genesis of the "force" constraint). Assuming the existence of a suitable function $\sigma(a)$, the conservation identity can be rewritten as

$$\sigma' = -\frac{2}{a} (\sigma + \mathcal{P}) + \Xi, \quad (11)$$

where $\sigma' = d\sigma/da$. The right hand side is the net discontinuity of the bulk momentum flux and is physically interpreted as the work done by external "forces" on the thin shell occurring due to $\Phi'_\pm \neq 0$. We can rearrange Eq.(6) into the form

$$\sqrt{1 - \frac{b_+(a)}{a} + \dot{a}^2} = -\sqrt{1 - \frac{b_-(a)}{a} + \dot{a}^2} - 4\pi a \sigma(a), \quad (12)$$

which yields the thin-shell equation of motion given by

$$\frac{1}{2}\dot{a}^2 + V(a) = 0, \quad (13)$$

where the potential $V(a)$ is given by

$$V(a) = \frac{1}{2} \left\{ 1 - \frac{\bar{b}(a)}{a} - \left[\frac{m_s(a)}{2a} \right]^2 - \left[\frac{\Delta(a)}{m_s(a)} \right]^2 \right\}, \quad (14)$$

$$\bar{b}(a) = \frac{b_+(a) + b_-(a)}{2}, \Delta(a) = \frac{b_+(a) - b_-(a)}{2}.$$

The potential $V(a)$ is seen as a function of the thin-shell mass $m_s(a) = 4\pi a^2 \sigma(a)$ and is the key for stability analysis. It follows from Eq.(14) that

$$m_s(a) = -a \left[\sqrt{1 - \frac{b_+(a)}{a} - 2V(a)} + \sqrt{1 - \frac{b_-(a)}{a} - 2V(a)} \right], \quad (15)$$

the negative sign is required for compatibility with the Lanczos equations (5). Assume a static solution (at a_0) to the equation of motion $\frac{1}{2}\dot{a}^2 + V(a) = 0$, then a Taylor expansion of $V(a)$ around a_0 to second order yields

$$V(a) = V(a_0) + V'(a_0)(a - a_0) + \frac{1}{2}V''(a_0)(a - a_0)^2 + O[(a - a_0)^3]. \quad (16)$$

But since we are expanding around a static solution, $\dot{a}_0 = \ddot{a}_0 = 0$, we automatically have $V(a_0) = V'(a_0) = 0$, so it is sufficient to consider

$$V(a) = \frac{1}{2}V''(a_0)(a - a_0)^2 + O[(a - a_0)^3]. \quad (17)$$

The static solution at a_0 is stable if and only if $V''(a_0) \geq 0$. Since $V(a_0) = 0$, it follows from Eq.(15) that

$$m_s(a_0) = -a_0 \left\{ \sqrt{1 - \frac{b_+(a_0)}{a_0}} + \sqrt{1 - \frac{b_-(a_0)}{a_0}} \right\}. \quad (18)$$

Linearized stability using the condition $V''(a_0) \geq 0$ leads to an inequality on $m_s''(a)|_{a_0}$, that is called the "mass" constraint given by

$$m_s''(a)|_{a_0} \geq \frac{1}{4a_0^3} \left[\frac{[b_+(a_0) - a_0 b'_+(a_0)]^2}{[1 - b_+(a_0)/a_0]^{3/2}} + \frac{[b_-(a_0) - a_0 b'_-(a_0)]^2}{[1 - b_-(a_0)/a_0]^{3/2}} \right] + \frac{1}{2} \left[\frac{b''_+(a_0)}{\sqrt{1 - b_+(a_0)/a_0}} + \frac{b''_-(a_0)}{\sqrt{1 - b_-(a_0)/a_0}} \right]. \quad (19)$$

Assuming integrability of Eq.(11), lengthy calculations yield the parametric solution: $\sigma \equiv \sigma(a)$, $\mathcal{P} \equiv \mathcal{P}(a)$ and $\Xi \equiv \Xi(a)$. The same linearized stability analysis with $V''(a_0) \geq 0$ also yields inequalities on σ' , σ'' , \mathcal{P}' , \mathcal{P}'' , Ξ' , Ξ'' but the last one is the most relevant. When $\Phi_{\pm} \neq 0$, there will appear an additional constraint analogous to the one on $m_s''(a)|_{a_0}$, called the "force" constraint given by

$$\begin{aligned} [4\pi \Xi(a) a]''|_{a_0} \leq & \left\{ \Phi_+'''(a) \sqrt{1 - b_+(a)/a} + \Phi_-'''(a) \sqrt{1 - b_-(a)/a} \right\} \Big|_{a_0} \\ & - \left\{ \Phi_+''(a) \frac{(b_+(a)/a)'}{\sqrt{1 - b_+(a)/a}} + \Phi_-''(a) \frac{(b_-(a)/a)'}{\sqrt{1 - b_-(a)/a}} \right\} \Big|_{a_0} \\ & - \frac{1}{4} \left\{ \Phi_+'(a) \frac{[(b_+(a)/a)]^2}{[1 - b_+(a)/a]^{3/2}} + \Phi_-'(a) \frac{[(b_-(a)/a)]^2}{[1 - b_-(a)/a]^{3/2}} \right\} \Big|_{a_0} \\ & - \frac{1}{2} \left\{ \Phi_+'(a) \frac{(b_+(a)/a)''}{\sqrt{1 - b_+(a)/a}} + \Phi_-'(a) \frac{(b_-(a)/a)''}{\sqrt{1 - b_-(a)/a}} \right\} \Big|_{a_0}. \end{aligned} \quad (20)$$

The same force constraint appears for $\Phi'_{\pm}(a_0) \leq 0$ as well but with only the sign in the inequality *reversed*. The three inequalities, (19),(20) and the reversed one, are the GLV master inequalities for deciding stability zones of thin-shell motion.

III. STABILITY OF THIN-SHELL FROM SCHWARZSCHILD BLACK HOLE- $f(R)$ WORMHOLE GLUING

(a) Schwarzschild black hole-MH1 wormhole

We glue at a common radius a_0 above the Schwarzschild horizon $r_{\text{hor}} = 2M$ and wormhole throat r_0 , i.e., at a certain radius $r = a_0 > 2M, r_0$. The interior regions $r \leq 2M, r_0$ are surgically excised out of the respective spacetimes because we don't want the presence of any horizon in the resultant wormhole. Thus linear spherical perturbations will be assumed to take place about the radius a_0 . Casting the Schwarzschild metric into the GLV form of Eq.(1), one obtains

$$b_+ = 2M, \quad \Phi_+ = 0, \quad (21)$$

and similarly casting the first metric of MH1 wormhole [1] of $f(R)$ -gravity, viz.,

$$d\tau^2 = - \left(1 + \frac{r_0}{r}\right)^{-2} dt^2 + \frac{dr^2}{1 - \frac{r_0^2}{r^2}} + r^2(d\theta^2 + \sin^2\theta d\phi^2), \quad (22)$$

in the form of GLV metric, we get

$$b_- = \frac{r_0^2}{r}, \quad \Phi_- = -\frac{1}{2} \ln \left[\left(1 - \frac{r_0}{r}\right) \left(1 + \frac{r_0}{r}\right)^3 \right]. \quad (23)$$

The redshift function $\Phi_-(r)$, now denoted without subscript simply as $\Phi(r)$, happens to be a logarithmic function showing divergence at $r = r_0$ but from the physical standpoint this does not pose any problem since we already made the choice that the accessible region has $r > r_0$ - the throat radius of the wormhole.

Stability zone of thin shell depends on the sign of $\Phi'(a_0)$, which for the MH1 solution is given by

$$\Phi'(a_0) = \frac{(a_0 - 2r_0)r_0}{(a_0^2 - r_0^2)a_0}. \quad (24)$$

There occurs two cases. Case 1: $r = a_0 \in (r_0, 2r_0]$, for which we get $\Phi'(a_0) \leq 0$ and Case 2: $r = a_0 \in [2r_0, \infty)$, for which we get $\Phi'(a_0) \geq 0$. In either case, there will occur the effect of external "force" influencing the thin shell motion. Introducing the above functions in the inequalities (19,20), and defining the dimensionless variables

$$x = \frac{M}{a_0}, \quad y = \frac{r_0}{M}, \quad (25)$$

we find, respectively

$$m_s''(a)|_{a_0} \geq f(x, y) = x \left(\frac{2}{\sqrt{1-2x}} + \frac{x}{(1-2x)^{3/2}} - \frac{xy^2(2x^2y^2-3)}{(1-x^2y^2)^{3/2}} \right), \quad (26)$$

$$[4\pi\Xi(a)a]''|_{a_0} \geq g_1(x, y) = \frac{xy(6-24xy-5x^2y^2+30x^3y^3+2x^4y^4-12x^5y^5)}{(1-x^2y^2)^{5/2}}, \quad (27)$$

$$(\Phi'_\pm(a_0) \leq 0, \text{ Case 1}) \quad (28)$$

$$[4\pi\Xi(a)a]''|_{a_0} \leq g_1(x, y). \quad (\Phi'_\pm(a_0) \geq 0, \text{ Case 2}) \quad (29)$$

It can be noticed from Eq.(26) that for $f(x, y)$ to be real, two conditions must be fulfilled: one is $x < \frac{1}{2}$, which implies $a_0 > 2M$ as required, and the other is $y < \frac{1}{x}$ or $a_0 > r_0$. The latter condition guarantees the reality of also $g_1(x, y)$. Note further that $y = \frac{r_0}{M}$ has no upper bound but has a lower bound 2 such that the wormhole throat satisfies $r_0 > 2M$ as required. The above Cases then split the xy plane into two areas: In Case 1, $x \in (\frac{1}{4}, \frac{1}{2})$, $y \in (2, 4)$ and in Case 2, $x \in (0, \frac{1}{4})$, $y \in (4, \infty)$. In the contour plots, the two areas are combined such that $x \in (0, \frac{1}{2})$, $y \in (2, \infty)$.

(b) Schwarzschild black hole-MH2 wormhole

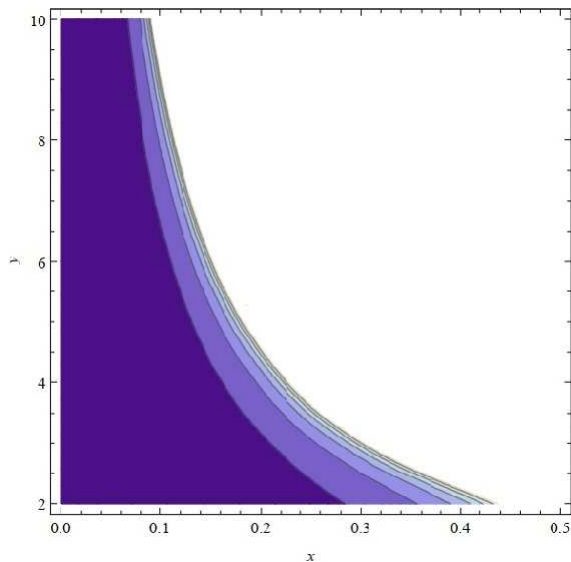


FIG. 1: 2D contour plot of $f(x, y)$ for $x \in (0, \frac{1}{2})$ and $y \in (2, \infty)$. The shaded region represents the zone of stability of the thin-shell exclusively under "mass constraint".

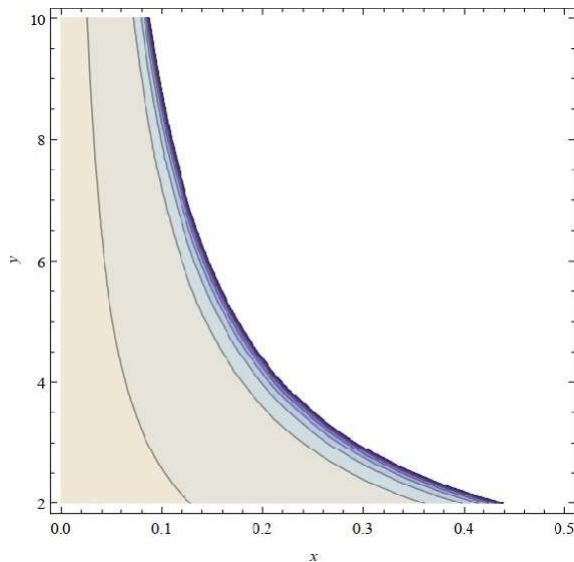


FIG. 2: 2D contour plot of $g_1(x, y)$. The relevant area is defined by $x \in (\frac{1}{4}, \frac{1}{2})$, $y \in (2, 4)$ in Case 1 [Sec.3(a)]. For Case 2 [Sec.3(a)], the relevant area is $x \in (0, \frac{1}{4})$, $y \in (4, \infty)$. In either case, the exclusive "force" constraint indicates that the shaded region is the stable zone.

The second wormhole MH2, cast in the GLV form, is

$$ds^2 = - \left(\frac{r}{r_0} \right)^4 dt^2 + \frac{dr^2}{1 - \frac{r_0^2}{r^2}} + r^2(d\theta^2 + \sin^2\theta d\phi^2), \quad (30)$$

$$b_- = \frac{r_0^2}{r}, \quad \Phi_- = \frac{1}{2} \ln \left[\frac{r^6}{r_0^4(r^2 - r_0^2)} \right]. \quad (31)$$

Like in (a), stability zone of the thin-shell depends on the sign of $\Phi'(a_0)$, which for the MH2 solution is given by

$$\Phi'(a_0) = \frac{2a_0^2 - 3r_0^2}{(a_0^2 - r_0^2)a_0}. \quad (32)$$

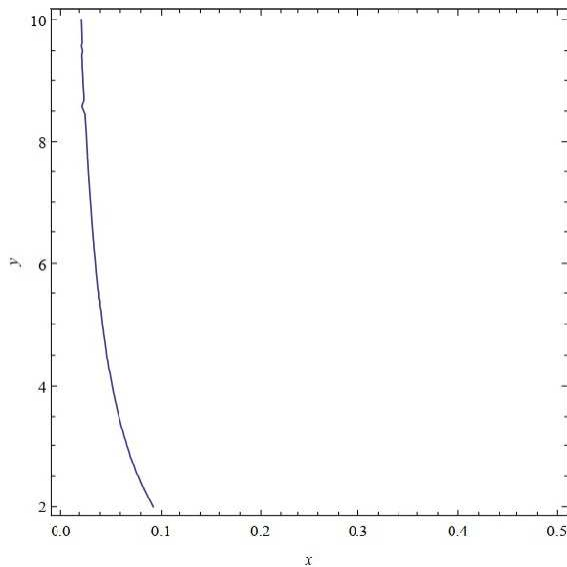


FIG. 3: Thin-shell stability under simultaneous constraints is restricted to parameter values (x, y) on the left of the curve obtained by the intersections $f(x, y) \cap g_1(x, y)$.

There again occurs two cases. Case 1: $r = a_0 \in (r_0, \sqrt{\frac{3}{2}}r_0]$, for which we get $\Phi'(a_0) \leq 0$ and Case 2: $r = a_0 \in [\sqrt{\frac{3}{2}}r_0, \infty)$, for which we get $\Phi'(a_0) \geq 0$. In either case, there will occur the effect of external "force" influencing the thin shell motion. These Cases, like in (a), will split the xy plane into two areas: In Case 1, $x \in (\frac{1}{\sqrt{6}}, \frac{1}{2})$, $y \in (2, \sqrt{6})$ and in Case 2, $x \in (0, \frac{1}{\sqrt{6}})$, $y \in (\sqrt{6}, \infty)$. In the contour plots to be given below, the two cases are combined such that $x \in (0, \frac{1}{2})$, $y \in (2, \infty)$. Introducing the above metric functions in the inequalities (19,20), we find

$$m_s''(a_0) \geq f(x, y) = x \left(\frac{2}{\sqrt{1-2x}} + \frac{x}{(1-2x)^{3/2}} + \frac{xy^2(2x^2y^2-3)}{(1-x^2y^2)^{3/2}} \right), \quad (33)$$

$$[4\pi\Xi(a)a]''|_{a_0} \geq g_2(x, y) = \frac{4 - 34x^2y^2 + 45x^4y^4 - 18x^6y^6}{(1-x^2y^2)^{5/2}}, \quad (34)$$

$$(\Phi'_{\pm}(a_0) \leq 0, \text{ Case 1}) \quad (35)$$

$$[4\pi\Xi(a)a]''|_{a_0} \leq g_2(x, y), \quad (\Phi'_{\pm}(a_0) \geq 0, \text{ Case 2}) \quad (36)$$

It can be seen that $f(x, y)$ in both (a) and (b) is the same, so exactly the same mass constraint applies to both. However, the functions $g_1(x, y)$ and $g_2(x, y)$ differ so that the force constraints differ. As a result, the combined effect of two constraints would also differ leading to different zones of stability. The results are discussed below.

IV. RESULTS AND DISCUSSION

The goal of this work was to demarcate the stability regions of the thin-shell formed by gluing the Schwarzschild black hole with $f(R)$ -gravity wormholes derived by MH. The remarkable feature of analytical MH wormholes is that they do not require elusive exotic matter but unfortunately are unstable. A limited stability ("graceful exit") can however be explored within the GLV formalism, which is robust providing an excellent way to tackle wider classes of thin-shell wormholes surgically born out of two static spherically symmetric spacetimes. The present study yields possible parameter ranges of the participating solutions (Schwarzschild-MH) for which stability in some sense can be achieved. Earlier, stability of thin-shell from Schwarzschild-Schwarzschild gluing using the approach of a potential was studied before by Poisson and Visser [43]. The stability constraints on the classes of thin-shells investigated here have relevance for their very existence, since stable *analytic* wormholes are rather scarce. The study of the properties

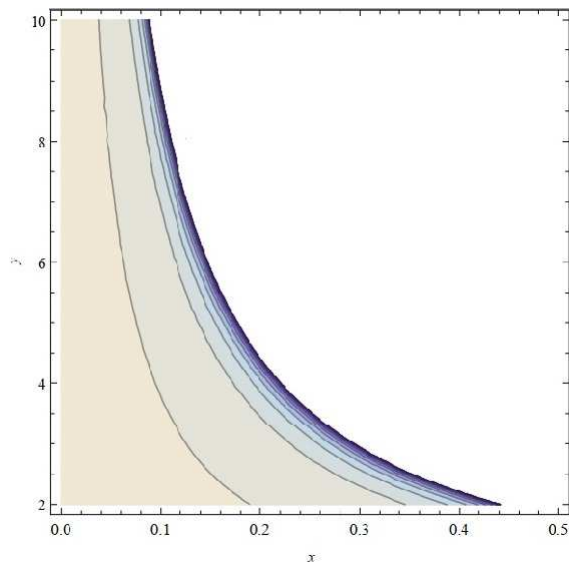


FIG. 4: 2D contour plot of $g_2(x, y)$. Qualitatively, the stability picture is the same as in Fig.2. For Case 1 [Sec.3(b)], the area of $g_2(x, y)$ is demarcated by $x \in (\frac{1}{\sqrt{6}}, \frac{1}{2})$, $y \in (2, \sqrt{6})$ and for Case 2 [Sec.3(b)], the relevant area is $x \in (0, \frac{1}{\sqrt{6}})$, $y \in (\sqrt{6}, \infty)$. The "force" constraint implies that the shaded area is the stable zone.

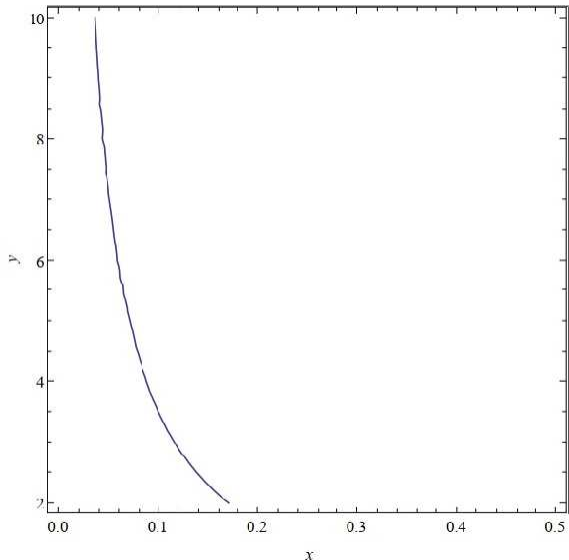


FIG. 5: Thin-shell stability under simultaneous constraints is restricted to parameter values (x, y) to the left of the curve obtained by the intersections $f(x, y) \cap g_2(x, y)$.

of light rings on either side of the shell would be interesting as a future task in connection with their characteristic ring-down modes [3-6].

The thin-shell examples considered above are interesting in their own right since by construction the exterior has a Schwarzschild vacuum ($M \neq 0$). Physically, this thin-shell configuration resembles a gravastar having an interior $f(R)$ -MH spacetime but the exterior vacuum is indistinguishable from the Schwarzschild black hole. The stability of the thin-shell is dictated by two constraints, one is "mass" constraint symbolized by an explicit inequality involving the second derivative of the mass of the throat, $m_s''(a_0)$ and the other is an external "force" constraint through the inequalities on $[4\pi \Xi(a) a]''$ depending on the signs of $\Phi'_\pm(a_0)$. Note that the "mass" constraint (19) does not involve Φ_\pm and its derivatives, while the "force" constraint (20 and its reverse) exists due to $\Phi_\pm \neq 0$. The latter constraint is a new discovery of GLV. Using these two constraints, we had demarcated the zones of stability in the parameter space.

The analyses in this paper bring out some important characteristics of Schwarzschild-MH thin-shell wormholes.

Even though the two independent MH wormholes have different metrics, the stability picture of thin-shells under discussion is remarkably similar. Especially, the contour for $f(x, y)$ is the same for both thin-shells since b_{\pm} are the same for both MH solutions, only the Φ_{\pm} are different. The variables for the contour plots are chosen as $x = \frac{M}{a_0}$, $y = \frac{r_0}{M}$, where $x \in (0, \frac{1}{2})$, $y \in (2, \infty)$, the ranges being dictated by the requirement that the gluing radius $a_0 > 2M$ and that the wormhole throat $r_0 > 2M$. The reality requirements of the functions $f(x, y)$, $g_1(x, y)$ and $g_2(x, y)$ yield parameter ranges $x < \frac{1}{2}$ and $y < \frac{1}{x}$. It is clear that as x increases from 0 to $\frac{1}{2}$, the gluing radius a_0 shrinks from ∞ to $2M$. Similarly, when y increases indefinitely from 2, the wormhole throat radius r_0 increases from $2M$ to ∞ .

The following are our new results. The shaded regions in the 2D contour plots represent the "topography" of the surfaces $f(x, y)$, $g_1(x, y)$ and $g_2(x, y)$. The higher values on the surfaces are marked by layers of lighter regions. The zones of stability depend on the Cases discussed in Sec.3. The "mass" constraint however does not involve such Cases as it does not involve Φ . Now consider (a) of Sec.3 analyzing Schwarzschild-MH1 thin-shell. The contour plot of the function $f(x, y)$ is given in Fig.1 for the parameter values $x \in (0, \frac{1}{2})$ and $y \in (2, \infty)$. The condition (26) then implies that the shaded region in Fig.1 is the zone of stability. The same conclusion holds for (b) too, i.e., for Schwarzschild-MH2 thin-shell.

The contour plot of the surface $g_1(x, y)$ is given in Fig.2, where the "force" constraint is divided also into two cases as pointed out in Sec.3(a). For Case 1, the area is demarcated by $x \in (\frac{1}{4}, \frac{1}{2})$, $y \in (2, 4)$ and for Case 2, area is defined by $x \in (0, \frac{1}{4})$, $y \in (4, \infty)$. (Note that the lines inside plots make boundaries of points of same heights and not the boundaries of the areas mentioned here). In either case, the shaded region in Fig.2 indicates the stability zone purely due to "force" constraint. The contour plot of the surface $g_2(x, y)$ is given in Fig.4 and again there occurs two Cases of inequalities as pointed out in Sec.3(b). Qualitatively, the stability picture is similar. For Case 1, the area is demarcated by $x \in (\frac{1}{\sqrt{6}}, \frac{1}{2})$, $y \in (2, \sqrt{6})$ and for Case 2, area is $x \in (0, \frac{1}{\sqrt{6}})$, $y \in (\sqrt{6}, \infty)$ implying that the shaded area in Fig.4 is the stable zone. However, the individual constraints do not completely describe the zones of stability.

The complete stability zone should be determined by the *combined* application of "mass" and "force" constraints. In this case, the stability zone is restricted to parameter values (x, y) on the left of the curves obtained by the intersections $f(x, y) \cap g_1(x, y)$ (Fig.3) and $f(x, y) \cap g_2(x, y)$ (Fig.5) respectively. The interesting result that follows from it is that Schwarzschild-MH2 thin-shell has a larger stability zone (Fig.5) than that of Schwarzschild-MH1 (Fig.3). The intriguing result that emerges is that the thin-shell motion is stable for $x < 0.1$ (Fig.3) and for $x < 0.2$ (Fig.5), i.e., when the gluing radius a_0 is rather far away from the horizon $a_0 = 2M$ or $x = \frac{1}{2}$. It can be verified that all the above stability zones can be read off from the 3D plots as well. Such a complete stability picture is possible essentially due to the effect of the "external force" constraint, a new discovery by GLV.

Acknowledgments

The reported study was funded by RFBR according to the research project No. 18-32-00377.

-
- [1] S.H. Mazharimousavi and M. Halilsoy, Mod. Phys. Lett. A **31**, 1650192 (2016).
 - [2] M.S. Morris and K.S. Thorne, Am. J. Phys. **56**, 395 (1988).
 - [3] V. Cardoso, E. Franzin and P. Pani, Phys. Rev. Lett. **116**, 171101 (2016); **117**, 089902E (2016).
 - [4] V. Cardoso and P. Pani, Nature Astronomy **1**, 586 (2017).
 - [5] R.A. Konoplya and A. Zhidenko, JCAP **12** (2016) 043.
 - [6] K.K. Nandi, R. N. Izmailov, A.A. Yanbekov and A.A. Shayakhmetov, Phys. Rev. D **95**, 104011 (2017).
 - [7] D. Hochberg and M. Visser, Phys. Rev. Lett. **81**, 746 (1998).
 - [8] S. Nojiri and S.D. Odintsov, Phys. Rev. D **74**, 086005 (2006).
 - [9] S.H. Mazharimousavi and M. Halilsoy, Phys. Rev. D **84**, 0640328 (2011);
A. Sheykhi, Phys. Rev. D **86**, 024013 (2012);
M. Cvetič, S. Nojiri and S.D. Odintsov, Nucl. Phys. B **628**, 295 (2002);
R.G. Cai, Phys. Rev. D **65**, 084014 (2002).
 - [10] A. de la Cruz-Dombriz and A. Dobado, Phys. Rev. D **74**, 087501 (2006);
A. de la Cruz-Dombriz, A. Dobado and A.L. Maroto, Phys. Rev. D **80**, 124011 (2009); Phys. Rev. D **83**, 029903E (2011);
A. de la Cruz-Dombriz, A. Dobado and A.L. Maroto, Phys. Rev. Lett. **103**, 179001 (2009);
P.K.S. Dunsby, V.C. Busti, S. Kandhai, Phys. Rev. D **89**, 064029 (2014);
J.A.R. Cembranos, A. de la Cruz-Dombriz and P. Jimeno Romero, Int. J. Geom. Meth. Mod. Phys. **11**, 1450001 (2014);
A. de la Cruz-Dombriz, P.K.S. Dunsby, S. Kandhai, D. Sáez-Gómez, Phys. Rev. D **93**, 084016 (2016).
 - [11] G.J. Olmo and D. Rubiera-Garcia, Phys. Rev. D **84**, 124059 (2011);
D. Bazeia, L. Losano, G.J. Olmo and D. Rubiera-Garcia, Phys. Rev. D **90**, 044011 (2014);

- E. Barrientos, F.S.N. Lobo, S. Mendoza, G.J. Olmo and D. Rubiera-Garcia, Phys. Rev. D **97**, 104041 (2018);
D. Bazeia, L. Losano, R. Menezes, G.J. Olmo and D. Rubiera-Garcia, Eur. Phys. J. C **75**, 569 (2015).
- [12] R. Goswami, A.M. Nzioki, S.D. Maharaj and S.G. Ghosh, Phys. Rev. D **90**, 084011 (2014);
A.M. Nzioki, R. Goswami and P.K.S. Dunsby, Int. J. Mod. Phys. D **26**, 1750048 (2016);
A.M. Nzioki, S. Carloni, R. Goswami and P.K.S. Dunsby, Phys. Rev. D **81**, 084028 (2010);
A.M. Nzioki, P.K.S. Dunsby, R. Goswami and S. Carloni, Phys. Rev. D **83**, 024030 (2011);
T. Clifton, P. Dunsby, R. Goswami and A.M. Nzioki, Phys. Rev. D **87**, 063517 (2013).
- [13] T.P. Sotiriou and V. Faraoni, Rev. Mod. Phys. **82**, 451 (2010).
- [14] S. Nojiri and S.D. Odintsov, Phys. Rept. **505**, 59 (2011).
- [15] S. Capozziello and V. Faraoni, *Beyond Einstein gravity*, Fundamental Theories of Physics 170 (Springer, 2011).
- [16] L. Sebastiani and S. Zerbini, Eur. Phys. J. C **71**, 1591 (2011).
- [17] S.E.P. Bergliaffa and Y.E.C. de O. Nunes, Phys. Rev. D **84**, 084006 (2011).
- [18] S.H. Mazharimousavi and M. Halilsoy, Phys. Rev. D **86**, 088501 (2012).
- [19] S.H. Mazharimousavi, M. Kerachian and M. Halilsoy, Int. J. Mod. Phys. D **22**, 1350057 (2013).
- [20] Y.S. Myung, T. Moon and E.J. Son, Phys. Rev. D **83**, 124009 (2011).
- [21] A.D. Dolgov and M. Kawasaki, Phys. Lett. B **573**, 1 (2003).
- [22] G.J. Olmo, Phys. Rev. Lett. **95**, 261102 (2005).
- [23] V. Faraoni and S. Nadeau Phys. Rev. D **72**, 124005 (2005).
- [24] G.J. Olmo, Phys. Rev. D **72**, 083505 (2005); D **75**, 023511 (2007).
- [25] Y.S. Myung, Eur. Phys. J. C **71**, 1550 (2011).
- [26] Y.S. Myung, Phys. Rev. D **88**, 104017 (2013).
- [27] A.M. Nzioki, R. Goswami and P.K.S. Dunsby, Phys. Rev. D **89**, 064050 (2014).
- [28] S.H. Mazharimousavi and M. Halilsoy, Phys. Rev. D **84**, 064032 (2011).
- [29] S.H. Mazharimousavi, M. Halilsoy and T. Tahamtan, Eur. Phys. J. C. **72**, 1851 (2012).
- [30] S. Soroushfar, R. Saffari and N. Kamvar, Eur. Phys. J. C **76**, 476 (2016).
- [31] Y. Yokokura, Int. J. Mod. Phys. A **27**, 1250160 (2012).
- [32] F.S.N. Lobo and M.A. Oliveira, Phys. Rev. D **80**, 104012 (2009).
- [33] S. Bhattacharya and S. Chakraborty, Eur. Phys. J. C **77**, 558 (2017).
- [34] C. Bambi, A. Cardenas-Avendano, G.J. Olmo and D. Rubiera-Garcia, Phys. Rev. D **93**, 064016 (2016).
- [35] S.H. Mazharimousavi and M. Halilsoy, Mod. Phys. Lett. A **31**, 1650203 (2016).
- [36] F. S. N. Lobo and P. Crawford, Class. Quant. Grav. **22**, 4869 (2005);
E.F. Eiroa, M.G. Richarte and C. Simeone, Phys. Lett. A **373**, 1 (2008);
E.F. Eiroa and G.F. Aguirre, Eur. Phys. J. C **76**, 132 (2016); Phys. Rev. D **94**, 044016 (2016).
- [37] E. F. Eiroa and C. Simeone, Phys. Rev. D **70**, 044008 (2004); Phys. Rev. D **71**, 127501 (2005);
F. Rahaman, M. Kalam and S. Chakraborti, Int. J. Mod. Phys. D **16**, 1669 (2007);
Z. Amirabi, M. Halilsoy, S.H. Mazharimousavi, Mod. Phys. Lett. A **33**, 1850049 (2018);
S.D. Forghani, S.H. Mazharimousavi and M. Halilsoy, Eur. Phys. J. C **78**, 469 (2018);
S.H. Mazharimousavi, M. Halilsoy and S.N.H. Amen. Int. J. Mod. Phys. D **26**, 1750158 (2017);
S.H. Mazharimousavi and M. Halilsoy, Int. J. Mod. Phys. D **27**, 1850028 (2017);
A. Eid, Indian J. Phys. **92**, 1065 (2018).
- [38] A.R. Khaybullina, G.F. Akhtaryanova, R.F. Mingazova, D. Saha and R.N. Izmailov, Int. J. Theor. Phys. **53**, 1590 (2014);
J.P.S. Lemos and F.S.N. Lobo, Phys. Rev. D **78**, 044030 (2008).
- [39] K.A. Bronnikov, M.V. Skvortsova and A.A. Starobinsky, Grav. Cosmol. **16**, 216 (2010).
- [40] N.M. Garcia, F.S.N. Lobo and M. Visser, Phys. Rev. D **86**, 044026 (2012).
- [41] N. Deruelle, M. Sasaki and Y. Sendouda, Prog. Theor. Phys. **119**, 237 (2008).
- [42] M. Visser, *Lorentzian Wormholes-From Einstein To Hawking* (AIP, New York, 1995).
- [43] E. Poisson and M. Visser, Phys. Rev. D **52**, 7318 (1995).